Available online at www.sciencedirect.com
ScienceDirect
Surface Science xxx (2008) xxx–xxx
SURFACE SCIENCE
www.elsevier.com/locate/susc

Surface segregation of gold for Au/Pd(1 1 1) alloys measured by low-energy electron diffraction and low-energy ion scattering

Zhenjun Li [a], Octavio Furlong [a], Florencia Calaza [a], Luke Burkholder [a], Hin Cheuk Poon [b], Dilano Saldin [b], Wilfred T. Tysoe [a,*]

[a] *Department of Chemistry and Biochemistry, and Laboratory for Surface Studies, University of Wisconsin-Milwaukee, Milwaukee, WI 53211, USA*
[b] *Department of Physics, and Laboratory for Surface Studies, University of Wisconsin-Milwaukee, Milwaukee, WI 53211, USA*

Received 10 October 2007; accepted for publication 7 January 2008

Abstract

The surface composition of a Au/Pd(1 1 1) alloy formed by depositing five monolayers of gold onto clean Pd(1 1 1) at 300 K in an ultrahigh vacuum and heating to various temperatures is measured from an analysis of the low-energy electron diffraction (LEED) intensity versus energy curves and by low-energy ion scattering (LEIS). The LEIS and LEED data yield values of the outer-layer gold coverage that are in good agreement and LEED shows that the second-layer gold concentration is intermediate between that of the surface and bulk. Plotting the gold coverage versus the bulk gold mole fraction estimated using Auger spectroscopy, clearly indicates that gold preferentially segregates to the surface and can be modeled by a simple Langmuir–McClean equation. A fit to the experimental data yields a value of the equilibrium constant for segregation of 3.2 ± 0.4, in good agreement with the value of 5.4 ± 0.2 obtained for Au/Pd(1 1 1) alloys grown on Mo(1 1 0) substrates.

Keywords: Gold; Palladium; Alloy; Low-energy ion scattering; Low-energy electron diffraction

1. Introduction

Palladium–gold bimetallic alloys have been found to provide both active and selective catalysts for a number of reactions including CO oxidation, cyclotrimerization of acetylene to benzene, vinyl acetate synthesis, selective oxidation of alcohols to aldehydes or ketones, oxidation of hydrogen to hydrogen peroxide, and hydrocarbon hydrogenation [1–10]. They are ideal systems for fundamental study since gold and palladium are completely miscible in all proportions with only a slight lattice mismatch (~4.9%) [11].

There are a number of strategies for preparing model Au/Pd(1 1 1) alloys. They can be synthesized by depositing various amounts of gold and palladium onto a Mo(1 1 0) substrate [12]. In this case, the alloys form a (1 1 1) structure on the molybdenum template and the alloy is produced by heating above ~800 K. Alternatively, several monolayers of gold are evaporated onto a Pd(1 1 1) substrate, which is heated to allow the gold to diffuse into the bulk to form the alloy [1,2,13–15]. The advantage of the latter approach is that it allows a wide range of alloy compositions to be obtained in a single experiment merely by heating the sample to various temperatures, while the former method requires different film compositions to be prepared for each alloy. A key issue in understanding the relationship between the composition and the surface chemistry of these alloys is a precise knowledge of the surface coverage of gold or palladium as a function of the mole fraction of each of the elements in the bulk of the alloy, as well as the distribution of gold and palladium atoms on the surface.

Since gold has a lower surface energy than palladium (the surface free energy of palladium is 2.05 J/m^2 [16],

* Corresponding author. Tel.: +1 414 229 5222; fax: +1 414 229 5036.
E-mail address: wtt@uwm.edu (W.T. Tysoe).

0039-6028/$ - see front matter © 2008 Published by Elsevier B.V.
doi:10.1016/j.susc.2008.01.019

and that of gold is 1.63 J/m^2 [17]), gold is expected to preferentially segregate to the surface, and this is indeed found experimentally [12]. In addition, both density functional theory (DFT) [18,19] and Monte Carlo [18] simulations suggest that the gold and palladium are not randomly distributed on the surface and that there is a net repulsive interaction between gold atoms in the alloy that leads to a larger proportion of isolated atoms than would be expected from a random distribution. Finally, it has been suggested that the surface composition of the alloy can be affected by the presence of adsorbates [20].

Surface spectroscopic techniques such as Auger or X-ray photoelectron spectroscopy have been used to try to establish the coverage of gold and palladium at the surface of Au/Pd(1 1 1) alloys [1,2,13–15] but, while these techniques are surface sensitive, they probe the first few layers and therefore give an average composition in the near-surface region rather than the composition of the outermost layer, which is the most important for understanding the surface chemistry. Low-energy ion scattering (LEIS) is inherently sensitive to just the outermost layer [21–23] and has been used to measure the relationship between the bulk and surface compositions of alloys grown on Mo(1 1 0) [12]. Low-energy electron diffraction (LEED), while not necessarily sensitive to just the outermost layer, is carried out using electron energies of ~150 eV where the electron mean-free path is close to its minimum value and so is the electron-based technique that is the most surface sensitive. Furthermore, by measuring the intensities versus beam energies of the diffraction spots from the alloy, these data can be analyzed to determine the composition of not only the outermost layer, but also that of second and deeper layers and, as such, provides complementary and somewhat more detailed information on the composition of the alloy. The following manuscript reports on the results of low-energy ion scattering (LEIS) and low-energy electron diffraction (LEED) measurements of gold–palladium alloys formed by evaporating five monolayers of gold onto a Pd(1 1 1) substrate and heating to various temperatures.

2. Experimental methods

The Pd(1 1 1) sample (1 cm diameter, 0.5 mm thick) was cleaned using a standard procedure, which consisted of cycles of argon ion bombardment (2 kV, 1 μA/cm^2) and annealing in 4×10^{-8} Torr of O_2 at 1000 K [24]. The cleanliness of the sample was judged using X-ray photoelectron spectroscopy (XPS) and oxygen titration where O_2 instead of CO desorbs following O_2 adsorption when the sample is carbon free. Gold was evaporated from a small alumina tube furnace [25]. In order to precisely control the temperature of gold, and therefore its evaporation rate, a C-type thermocouple was placed into the gold pellet. It has been found that controlled and reproducible evaporation rates can be achieved by maintaining a constant furnace temperature. Prior to evaporation, the gold source was extensively outgassed at 1300 K for several hours. During gold evaporation, the chamber pressure was maintained below 8×10^{-10} Torr.

X-ray photoelectron spectra (XPS), for monitoring sample cleanliness, were collected in a UHV chamber operating at a base pressure of 2×10^{-10} Torr, described previously [26]. Both the LEED and LEIS experiments were carried out in an ultrahigh vacuum chamber operating at a base pressure of $\sim 1 \times 10^{-10}$ Torr following bakeout. The inner walls of this chamber contain two layers of μ-metal to exclude magnetic fields. The chamber was configured to include a four-grid, retarding-field analyzer with integral electron gun to collect LEED I/E curves as described previously [27,28]. For LEIS experiments, the chamber was configured to include a 50-mm diameter hemispherical analyzer capable of energy analyzing ions, and an inert gas ion source. Experiments were carried out using 1080 eV helium ions (He^+) with a scattering angle of 90°. The analyzer was operated at a pass energy of 90 eV to maximize the ion count rate and was under computer control using LabView software to vary the analyzer energy and measure ion counts rates. The LEIS spectra were collected for about 2 min to minimize effects of the ion beam on the sample and blank experiments were carried out to show that the composition varied by less than 5% during data collection. The gold coverage (denoted Θ_{Au}) on the Au/Pd(1 1 1) alloy surface was calculated using the equation [22]

$$\Theta_{Au} = \frac{I_{Au}}{(I_{Au} + f_{Au,Pd} I_{Pd})} \quad (1)$$

where I_{Au} and I_{Pd} are the integrated intensities under the scattering features for gold (at ~960 eV) and palladium (at ~927 eV), respectively, and $f_{Au,Pd}$ is a correction factor obtained from the integrated intensities of the gold feature for a five-monolayer evaporated film and the pure palladium surface.

3. Results

Both the LEED and LEIS experiments were carried out for alloys prepared using a standard set of experimental conditions, which involved depositing five monolayers of gold onto a Pd(1 1 1) single crystal at 300 K. Monolayer formation was gauged from the variation in gold and palladium XPS or Auger signal intensities as a function of deposition time [13–15]. As noted above, constant and reproducible deposition rates are obtained since the deposition geometry and pellet temperature are maintained constant. In the case of LEIS experiments (see below), the formation of the monolayer was also confirmed from the disappearance of signals due to the palladium substrate. In all cases, the sample was then sequentially heated to 600, 700, 800, 850, 900, 950 and 1100 K for 300 s, then allowed to cool to room temperature, following which the experiment was performed. Previous XPS analyses of the surface following this treatment confirm the formation of a gold–palladium alloy [13–15], consistent with the conclusions from other work [1,2]. Since Auger spectroscopy is

sensitive to the outermost several monolayers, the relative intensities of the Au NVV and Pd MNN signals were used to gauge the mole fractions of gold and palladium in the alloy.

3.1. Low-energy electron diffraction

The (1 × 1) LEED patterns of the initial gold surface and the intermediate Au/Pd(1 1 1) alloys were measured using an incident beam energy of 150 eV after annealing to the temperatures indicated above. It has been found that the lattice spacings for gold–palladium alloys vary linearly between that of pure gold and pure palladium as a function of composition [11]. The lattice spacings are measured from the separation of the LEED diffraction features and converted to composition assuming such a linear variation. The results are displayed in Fig. 1 and show a smooth variation with composition from pure gold to a surface enriched in palladium as a function of annealing temperature. The larger error bars for the data collected at lower temperatures arise since the surfaces are somewhat less ordered at these temperatures yielding less sharp diffraction spots. These results are in reasonable agreement with those of previous experiments [1,2].

The intensity versus beam energy (I/E) curves were measured for each of the alloys after annealing to the temperatures given above. The resulting data for the (0 1) and (1 0) beams are displayed in Figs. 2 and 3, respectively. The annealing temperatures are displayed adjacent to the corresponding spectra. For both sets of data, there are clear differences in the shapes of the I/E curves indicating that there are substantial changes in the nature of the surface and its composition, consistent with the formation of Au/Pd(1 1 1) alloys.

3.2. Low-energy ion scattering

Low-energy ion scattering data were collected for samples prepared using identical protocols as for the LEED data shown in Section 3.1. Thus, again, five monolayers of gold were deposited onto the Pd(1 1 1) surface and annealed to various temperatures. The areas under the scattering features due to gold (at ~960 eV) and palladium (at ~927 eV) were integrated, and the resulting gold coverage, calculated using Eq. (1), is plotted in Fig. 4 as a function of annealing temperature (■). This reveals that the

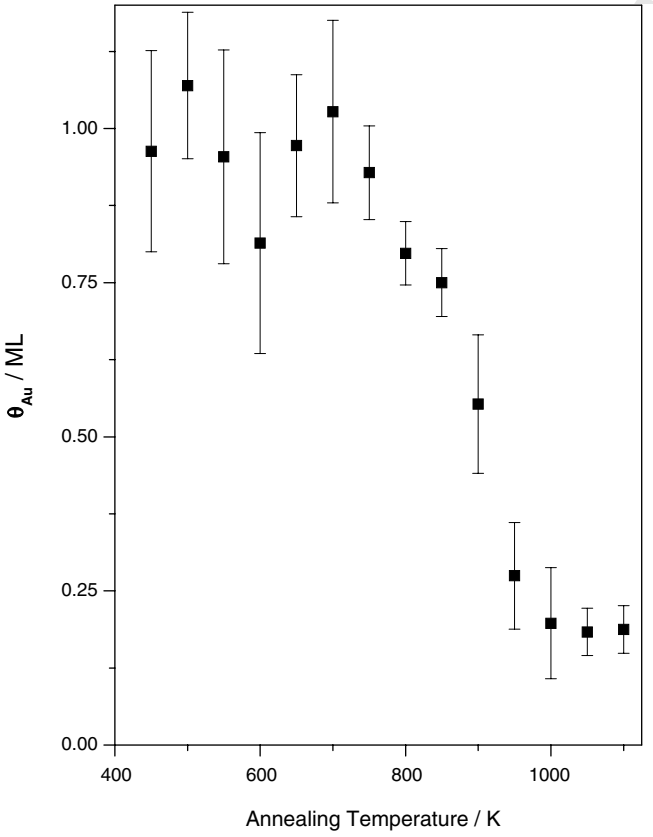

Fig. 1. Plot of the proportion of gold in the surface as a function of annealing temperature from the variation in lattice spacing measured by low-energy electron diffraction for five monolayers of gold deposited at 300 K on Pd(1 1 1).

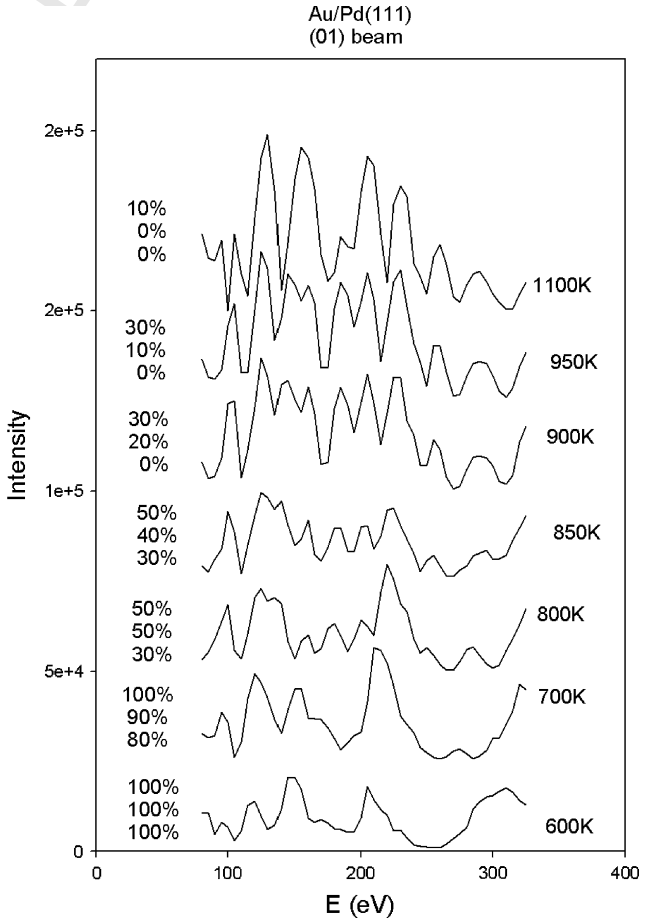

Fig. 2. LEED I/E curves of the (0 1) beam collected as a function of annealing temperature for five monolayers of gold deposited at 300 K on Pd(1 1 1) where the annealing temperatures are marked adjacent to the corresponding spectrum.

Please cite this article in press as: Z. Li et al., Surf. Sci. (2008), doi:10.1016/j.susc.2008.01.019

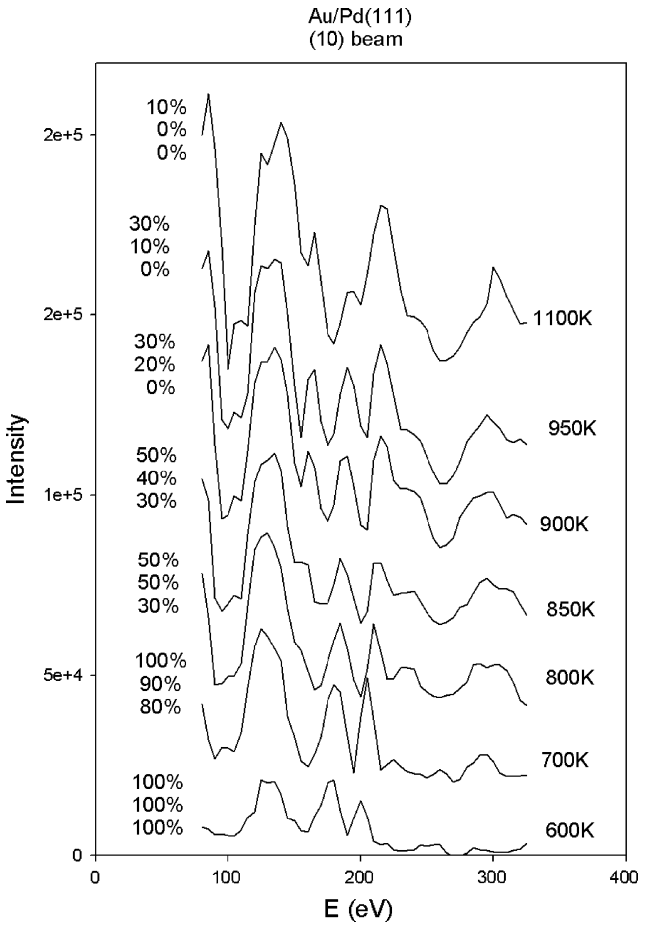

Fig. 3. LEED I/E curves of the (10) beam collected as a function of annealing temperature for five monolayers of gold deposited at 300 K on Pd(111) where the annealing temperatures are marked adjacent to the corresponding spectrum.

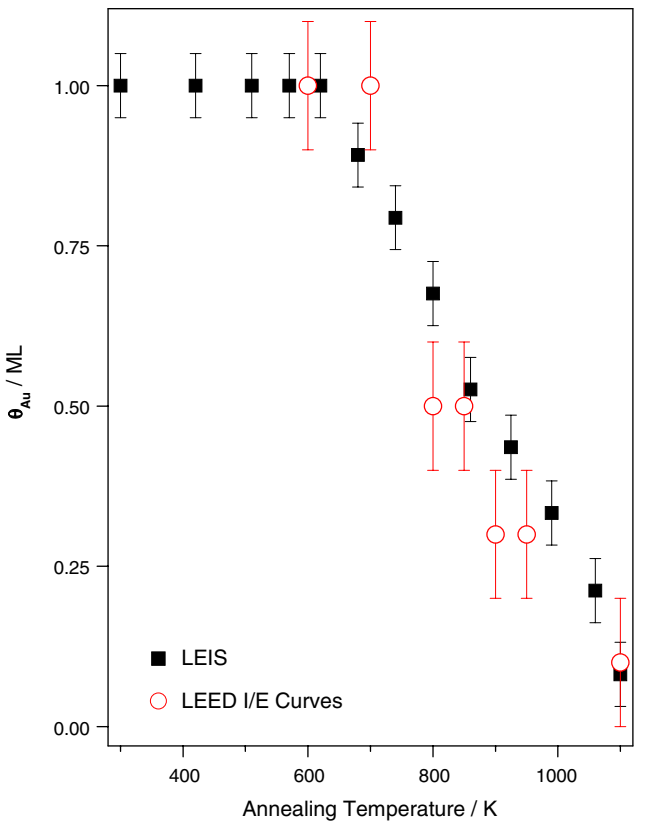

Fig. 4. Plot of the gold coverage for the Au/Pd(111) alloy as a function of annealing temperature (■) measured using low-energy ion scattering. Shown for comparison are the results of a LEED I/E analysis of the alloy (○).

gold coverage in the outermost layer does not start to diminish until the sample has been annealed to ~600 K, and does not decrease substantially until the sample has been heated to ~700 K. This is in accord with previous work [1,2] and also with the data of Fig. 1, which shows that the lattice spacing measured by LEED remains close to that of pure gold for annealing temperatures below ~700 K. In addition, after heating to ~1100 K, the measured lattice spacing yields a composition of ~20% gold (Fig. 1), while both the LEIS and LEED I/E analysis data suggest that the true gold coverage in the outermost layer is ~0.1 monolayers (Fig. 4).

4. Discussion

LEED measurements of the lattice spacing in the near-surface region (Fig. 1) indicate that the alloy starts to form on heating to ~700 K in accord with previous surface analytical measurements such as X-ray photoelectron spectroscopy [1,2]. However, the I/E curves shown in Figs. 2 and 3 can be analyzed to yield values of the gold coverage in the outermost and deeper layers. Theoretical LEED I/E curves were calculated for a wide range of gold palladium alloys by varying the gold coverage in the outermost layer (C1) and the second layer (C2) for varying bulk gold mole fractions (C3), which was assumed to be constant throughout the film. The theoretical I/E curves were calculated using a standard package [29] and each of the parameters were varied on the range 0, 0.2, 0.4, 0.6, 0.8 and 1.0. The Pendry R-factor [30] was then calculated for the experimental I/E curves obtained at each annealing temperature and displayed as contour plots versus C1 and C2 for various values of C3. A typical series of contour plots for a Au/Pd(111) alloy annealed to 800 K is displayed in Fig. 6 and calculations were carried out both for the (01) and (10) beams (see Figs. 2 and 3, respectively). The minimum Pendry R-factor was then read from these data to yield the optimal values of C1, C2 and C3 for each annealing temperature and the results are given adjacent to the respective I/E curves in Figs. 2 and 3 where the top number refers to C1, the second number to C2, and the bottom number to C3, and the error limits are estimated to be ±10%. The resulting values of the outermost layer coverage from LEED (C1, ○) are also compared with the results of the LEIS experiments (■) in Fig. 3, where the agreement is reasonable. However, the LEED I/E analysis provides additional information on the profile of gold within the near-

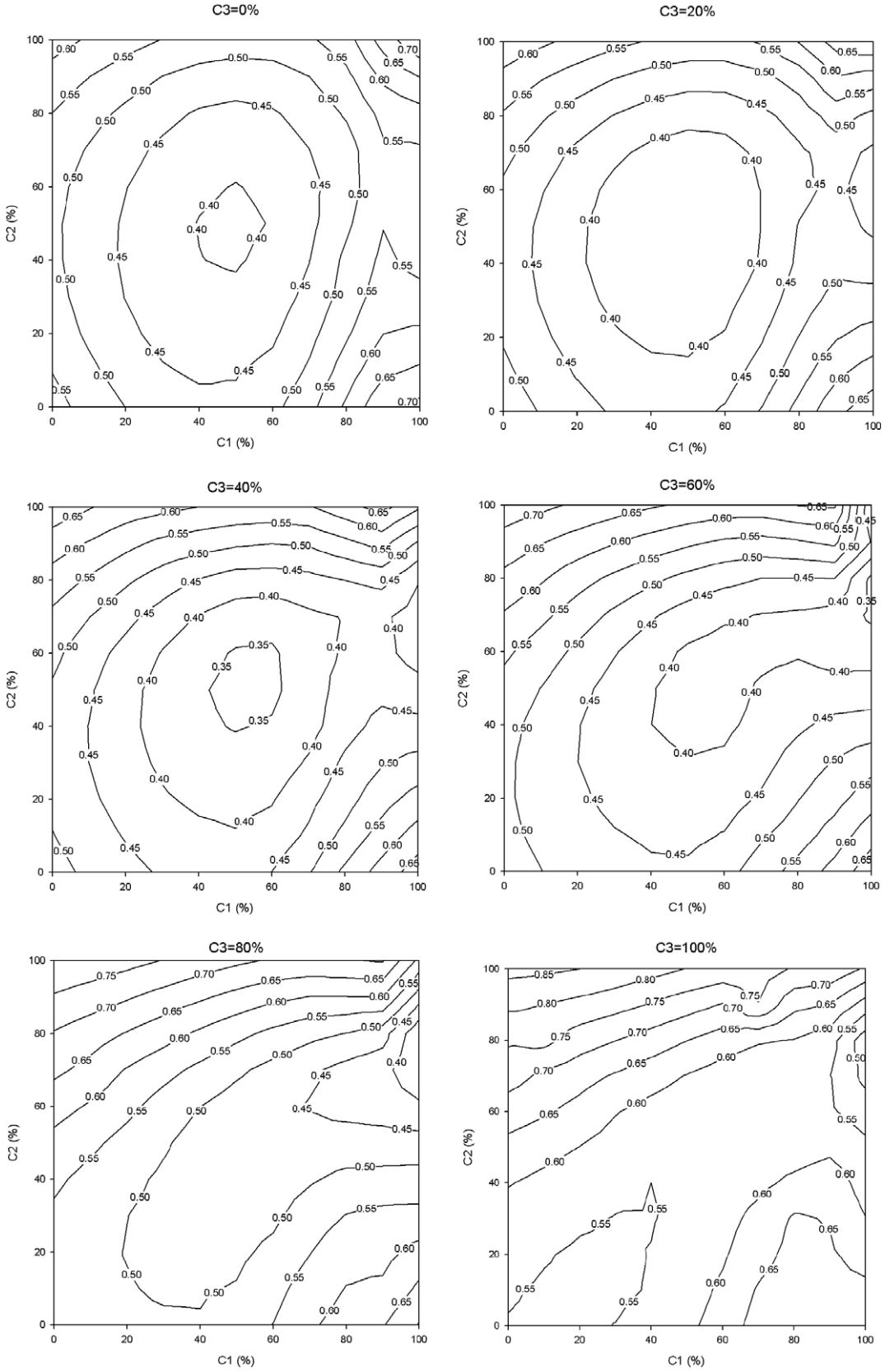

Fig. 5. Typical contour plots of the Pendry *R*-factor as a function of C1, the gold coverage in the outermost layer, C2 the gold coverage in the second layer for various bulk mole fractions of gold (C3), where the values of C3 are indicated for each plot.

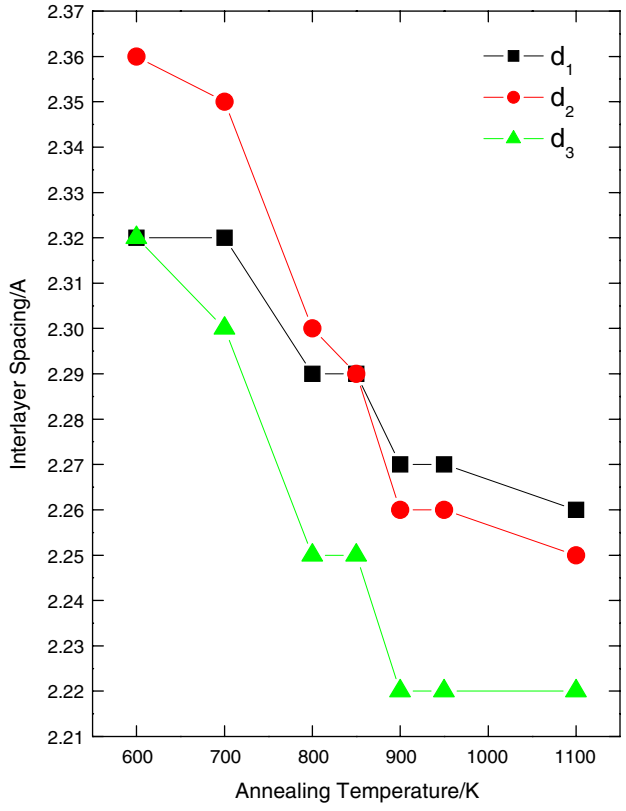

Fig. 6. Plot of interlayer spacing for the various alloys as a function of annealing temperature for d_1 (■), d_2 (●) and d_3 (▲), taken from the LEED I/E analysis (Table 2).

surface region and shows that the second-layer gold coverage is always lower than that in the outermost layer (Figs. 2 and 3).

The parameters used for the LEED I/E analysis are displayed in Table 1. The real part of the inner potential (V) is energy dependent due to exchange-correlation. The rate of change (dV/dE) was optimized for annealing temperatures of 600 K and 1100 K where the surface consists almost entirely of Au and Pd, respectively. The values of dV/dE at intermediate temperatures were interpolated according to the average concentration over all the layers. The phase shifts of Au and Pd depend on the vibration amplitudes, which in turn depend on the temperature. The surface and bulk vibration amplitudes of Au and Pd were optimized at 600 K and 1100 K and the amplitudes at intermediate temperatures were calculated according to the Debye model.

It has been shown that the bulk lattice spacing varies linearly with composition for gold palladium alloys [11]. To restrict the number of free parameters, only the interlayer spacings at 600 K and 1100 K were optimized. The interlayer spacings at intermediate temperatures were not optimized and were simply interpolated according to the average alloy concentration of the two layers involved. The interlayer spacings between the top and second layers (d_1), between the second and thirds layers (d_2), and for the bulk (d_3) are plotted versus annealing temperatures in Fig. 6. The lines shown on this plot are given as a guide to the eye. This shows that the lattice spacing decreases in going from a gold-rich surface to a palladium-rich surface, consistent with the larger lattice spacing for gold than palladium.

Finally, the gold coverages measured using LEIS (taken from the data in Fig. 4) are plotted versus the gold mole fraction in the alloy measured, in this case, using Auger spectroscopy in Fig. 7. Since this is sensitive to both the surface and the near-surface region, it is taken to be an estimate of the "bulk" alloy composition near the surface. Clearly from the results of the I/E analyses of the surface, the gold composition varies substantially in this region so that this value includes contributions from the top layer as well as layers near the surface. It should be noted that X-ray photoelectron spectroscopy analyses of the alloy composition yields almost identical results. In this case, intermediate alloy compositions are measured from the peak-to-peak intensities of the gold NVV and palladium MNN Auger features, which are corrected for their relative sensitivities measured using the five-monolayer gold film and the clean Pd(1 1 1) substrate.

This clearly reveals that the surface is considerably enriched in gold compared to the bulk since, if there were no preferential segregation, the graph would be a straight line. This result is in excellent agreement that found previously for gold palladium alloys [1,2,12]. Scanning-tunneling microscope images for an alloy that, from Auger spectroscopy measurements, contains a gold mole fraction of ~0.11, has a gold coverage of ~0.17 [31]. This result is also in good agreement with the data displayed in Fig. 7.

Table 1
Parameters used for the theoretical LEED I/E analyses for the gold palladium alloys formed by annealing to various temperatures

Temperature (K)	Average dV/dE	Vibration amplitude (Å)				R-factor
		Surface palladium	Bulk palladium	Surface gold	Bulk gold	
600	0			0.26	0.18	0.26
700	0.003	0.09	0.09	0.28	0.19	0.25
800	0.019	0.09	0.09	0.29	0.21	0.34
850	0.020	0.10	0.10	0.30	0.21	0.37
900	0.028	0.10	0.10	0.31	0.22	0.36
950	0.029	0.10	0.10	0.32	0.23	0.36
1100	0.032	0.11	0.11			0.18

Please cite this article in press as: Z. Li et al., Surf. Sci. (2008), doi:10.1016/j.susc.2008.01.019

Table 2
Values of the interlayer spacing used in the LEED I/E analyses of the various Au/Pd(1 1 1) alloys formed by annealing to various temperatures

Temperature (K)	d_1 (Å)	d_2 (Å)	d_3 (Å)
600	2.32	2.36	2.32
700	2.32	2.35	2.30
800	2.29	2.30	2.25
850	2.29	2.29	2.25
900	2.27	2.26	2.22
950	2.27	2.26	2.22
1100	2.26	2.25	2.22

Only the spacings at 600 K and 1100 K were optimized. The spacings at intermediate temperatures were interpolated according to the average concentration of the two layers involved. For example, d_1 at intermediate temperatures was estimated by interpolating the average Au concentrations of the first and second layers.

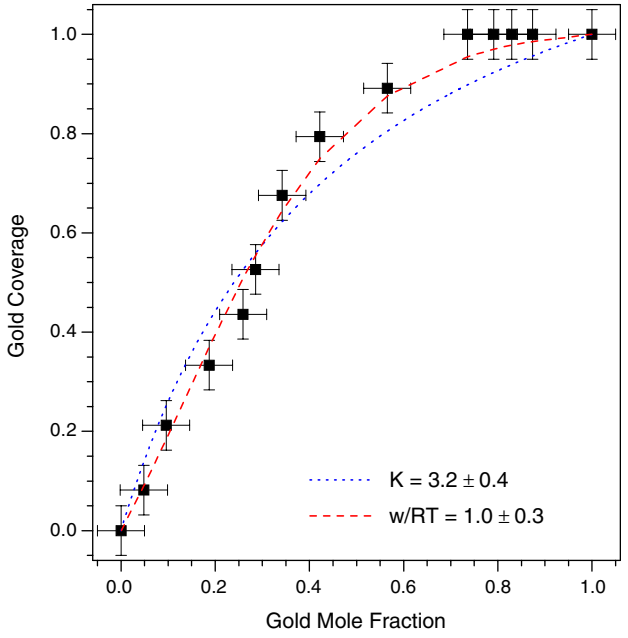

Fig. 7. Plot of the gold coverage at the surface of the alloy, measured by LEIS, against mole fraction of gold in the alloy measured using Auger spectroscopy (■). Shown plotted onto these data are theoretical curves (see text).

The most straightforward method for analyzing such data is to use the Langmuir–McClean equation [32], which assumes a simple equilibrium between the surface and bulk, yielding

$$\Theta(\mathrm{Au}) = \frac{KX(\mathrm{Au})}{1-(1-K)X(\mathrm{Au})} \qquad (2)$$

where Θ(Au) is the gold coverage at the surface of an alloy with a gold mole fraction X(Au), where the equilibrium constant is K. A fit to this function is shown plotted in Fig. 5 (—) and yields a value of $K = 3.2 \pm 0.4$. As noted above, Au/Pd(1 1 1) alloys have been grown previously on Mo(1 1 0) substrates where the bulk composition is controlled by the initial amount of gold and palladium that are deposited [12]. Similar LEIS experiments were carried out for various alloy compositions for Au/Pd/Mo(1 1 0). A fit to the Langmuir–McClean equation (2) for these data yields a value of $K = 5.4 \pm 0.2$, in reasonable agreement with that for the Au/P(1 1 1) alloys grown on a Pd(1 1 1) substrate measured here.

The simple Langmuir–McClean model for segregation only takes into account energy differences between gold in the bulk and surface. It has recently been demonstrated that there are effective repulsive interactions between gold and palladium atoms on a Au/Pd(1 1 1) alloy surface [18,19] such that there are significantly more isolated atoms on the surface than would be predicted from a simply random distribution [33]. If these interaction energies are relatively small, this effect can be treated using a simple Bragg–Williams approximation, so that K is given by

$$K = K_0 \exp\left(\frac{2wX(\mathrm{Au})}{RT}\right) \qquad (3)$$

where K_0 still depends on the segregation energy, and w is an energy corresponding to the difference in repulsive energies between gold and palladium in the bulk and on the surface. Note that the fit to the experimental data to the Langmuir–McClean equation (Eq. (1)) appears to underestimate the segregation at large gold mole fractions. The dashed line to the data in Fig. 7 is a fit to a Langmuir–McClean equation, modified by using Eq. (3) for K. This clearly leads to a substantial improvement in the fit to the experimental data and yields a value of $w/RT = 1.0 \pm 0.3$, where the relatively large error limits reflects the error in both gold coverage, measured by LEIS, and the gold mole fraction, measured by Auger spectroscopy. A similar fit to the data for gold–palladium alloys on a Mo(1 1 0) substrate [12] yields much lower values of $w/RT \sim 0.1$. However, recent Monte Carlo simulations of the distribution of gold and palladium in the alloy surface [18] reproduced the experimentally observed distribution on the alloy surface with a value of $w/RT = 0.64 \pm 0.12$, so that it is difficult to arrive at any firm conclusions regarding the magnitudes of the gold–palladium repulsions.

5. Conclusions

The coverage of gold within the outermost layer of a Au/Pd(1 1 1) alloy prepared by depositing five monolayers of gold onto a Pd(1 1 1) single crystal substrate is measured by a combination of an analysis of LEED I/E curves and LEIS. Both techniques show that there is a substantial enrichment of gold at the surface compared to the bulk composition as anticipated from the relative surface energies of gold and palladium. The results from the LEED I/E analysis are in reasonable agreement with the LEIS data, although they are much less accurate. They do, nevertheless, reveal that the second-layer composition is intermediate between that of the surface and the bulk of the alloy. The plot of surface coverage, measured from LEIS, versus the concentration of the alloy in the near-surface regions, measured from Auger spectroscopy, can be modeled

Please cite this article in press as: Z. Li et al., Surf. Sci. (2008), doi:10.1016/j.susc.2008.01.019

reasonably well using Langmuir–McClean theory with an equilibrium constant of 3.2 ± 0.4, in good agreement with the value of 5.4 ± 0.2 obtained for Au/Pd(1 1 1) alloys grown on Mo(1 1 0) substrates. Improvements in the fit to the experimental results are found when lateral interactions are taken into account using the Bragg–Williams approximation.

Acknowledgements

We gratefully acknowledge the support of this work by the US Department of Energy, Office of Basic Energy Sciences, under Grant Nos DE-FG02-92ER14289 (Division of Chemical Sciences, PI: WTT) and DE-FG02-84ER-45076 (Division of Materials Sciences and Engineering, PI: DKS).

References

[1] C.J. Baddeley, M. Tikhov, C. Hardacre, J.R. Lomas, R.M. Lambert, J. Phys. Chem. 100 (1996) 2189.
[2] C.J. Baddeley, R.M. Ormerod, A.W. Stephenson, R.M. Lambert, J. Phys. Chem. 99 (1995) 5146.
[3] Y.F. Han, D. Kumar, D.W. Goodman, J. Catal. 230 (2005) 353.
[4] A.M. Venezia, V. La Parola, B. Pawelec, J.L.G. Fierro, Appl. Catal. A 264 (2004) 43.
[5] M.S. Chen, D. Kumar, C.W. Yi, D.W. Goodman, Science 310 (2005) 291.
[6] L. Piccolo, A. Piednoir, J.-C. Bertolini, Surf. Sci. 592 (2005) 169.
[7] N. Dimitratos, A. Villa, D. Wang, F. Porta, D. Su, L. Prati, J. Catal. 244 (2006) 113.
[8] D.I. Enache, J.K. Edwards, P. Landon, B. Solsona-Espriu, A.F. Carley, et al., Science 311 (2006) 362.
[9] P. Landon, P.J. Collier, A.J. Papworth, C.J. Kiely, G.J. Hutchings, Chem. Commun. 18 (2002) 2058.
[10] J.K. Edwards, B.E. Solsona, P. Landon, A.F. Carley, et al., J. Catal. 236 (2005) 69.
[11] J. Banhart, Phys. Rev. B 53 (1996) 7128.
[12] C.W. Yi, K. Luo, T. Wei, D.W. Goodman, J. Phys. Chem. B 109 (2005) 18535.
[13] F. Calaza, F. Gao, Z. Li, W.T. Tysoe, Surf. Sci. 601 (2007) 714.
[14] Z. Li, F. Calaza, F. Gao, W.T. Tysoe, Surf. Sci. 601 (2007) 1351.
[15] Z. Li, F. Gao, Y. Wang, L. Burkholder, W.T. Tysoe, Surf. Sci. 601 (2007) 1898.
[16] L.Z. Mezey, J. Giber, Jpn. J. Appl. Phys. 11 (1982) 1569.
[17] W.R. Tyson, W.A. Miller, Surf. Sci. 62 (1977) 267.
[18] J.A. Boscoboinik, C. Plaisance, M. Neurock, W.T. Tysoe, Phys. Rev. B, in press. Q1
[19] D. Yuan, X. Gong, R. Wu, Phys. Rev. B 75 (2007) 087428.
[20] T.G. Owens, T.E. Jones, T.C.Q. Noakes, C.J. Baddeley, J. Phys. Chem. B 110 (2006) 21152.
[21] D.P. Woodruff, T.A. Delchar, Modern Techniques of Surface Science, second ed., Cambridge University Press, 1994.
[22] H. Niehus, W. Heiland, E. Taglauer, Surf. Sci. Rep. 17 (1993) 213.
[23] H.H. Brongersma, M. Draxler, M. de Ridder, P. Bauer, Surf. Sci. Rep. 62 (2007) 63.
[24] D. Stacchiola, L. Burkholder, W.T. Tysoe, Surf. Sci. 511 (2002) 215.
[25] W.J. Wytenburg, R.M. Lambert, J. Vac. Sci. Technol. A 10 (1992) 3597.
[26] Yilin Wang, Feng Gao, W.T. Tysoe, J. Mol. Catal. A-Chem. 236 (2005) 18.
[27] T. Zheng, W.T. Tysoe, H.C. Poon, D.K. Saldin, Surf. Sci. 543 (2003) 19.
[28] H.C. Poon, M. Weinert, D.K. Saldin, D. Stacchiola, T. Zheng, W.T. Tysoe, Phys. Rev. B 69 (2004) 035401.
[29] A. Barbieri, P.J. Rous, A. Wander, M.A. Van Hove, Automated Tensor LEED Programs Package, available from M.A. Van Hove. Q2
[30] J.B. Pendry, J. Phys. C 13 (1980) 937.
[31] B. Gleich, M. Ruff, R.J. Behm, Surf. Sci. 386 (1997) 48.
[32] J.M. Howe, Interfaces in Materials, John Wiley and Sons, New York, 1977.
[33] A.C. Clark, The Theory of Adsorption and Catalysis, Academic Press, New York, 1970.